Eur Biophys J (1993) 22:351–357

European Biophysics Journal

A refined three-dimensional solution structure of a carboxy terminal fragment of apolipoprotein CII

Anders Öhman, Per-Olof Lycksell, Astrid Gräslund

Department of Medical Biochemistry and Biophysics, University of Umeå, S-901 87 Umeå, Sweden

Received: 14 April 1993 / Accepted in revised form: 24 August 1993

Abstract. The three-dimensional structure of a synthetic fragment of human apolipoprotein CII (apo-CII) in 35%, 1,1,1,3,3,3-hexafluoro-2-propanol (HFP) has been determined on the basis of distance and intensity constraints derived from two-dimensional proton nuclear magnetic resonance measurements. The NOE crosspeak build-up rates were converted to distance constraints which were used in the distance geometry program DIANA. A set of one hundred structures were generated and of these ten structures were used in molecular dynamics simulations using the program XPLOR. This program enabled a direct minimization between the difference of the two-dimensional NOE intensities and those calculated from the full relaxation matrix. In this way spin diffusion is fully taken into account, which can be seen from the considerable improvement of the R-factor after the relaxation matrix refinement. These calculations show that this fragment, which corresponds to the carboxy terminal 30 amino acids of intact apo-CII and which retains its ability to activate lipoprotein lipase, is essentially flexible, but has three defined secondary structural elements. The most significant one is an α-helix between residues 67 and 74. The following three residues adopt a turn-like structure. Another turn of α-helix is seen between residues 56 and 59. The effect of the solvent system on the secondary structure was studied by circular dichroism spectroscopy. The results show that the mixed aqueous 35% HFP solvent induces secondary structure of a very similar nature to the one induced by sodium dodecyl sulphate.

Key words: Apolipoprotein CII – ^{1}H-NMR – Distance geometry – Molecular dynamics – Relaxation matrix refinement

Introduction

Human apolipoprotein CII (apo-CII) is a 79 amino acid residue protein which is bound to lipoprotein particles. Its role in metabolism is to activate the enzyme lipoprotein lipase, which hydrolyses triglycerides contained in lipoprotein particles. Apo-CII has two functional parts, the N-terminal part, up to approximately residue 50, functioning as an anchor to the lipoprotein particles, and the C-terminal part, functioning as the lipase activator (Wang 1991 and references cited therein).

This work concerns a fragment, which corresponds to the carboxy terminal 30 amino acid residues with a molecular weight of 3.3 kDa and which has full ability to activate lipoprotein lipase (Lycksell et al. 1992). Apo-CII has a limited solubility in water and is known to aggregate (Mantulin et al. 1980). The C-terminal fragment also exhibits self association in aqueous solution, observable through a badly resolved ^{1}H-NMR spectrum. Upon addition of 1,1,1,3,3,3-hexafluoro-2-propanol (HFP) the spectral resolution was found to increase considerably. Our recent NMR study in an aqueous solvent with 35% HFP (Lycksell et al. 1992) resulted in sequence specific assignment of the proton resonances and a proposed secondary structure. Based on these NMR-data the present study concerns the determination of a three dimensional solution structure by calculations using distance geometry, restrained molecular dynamics and refinement using a full relaxation matrix.

We have also addressed the question of how solvent interaction affects the average secondary structure in solution, by using circular dichroism (CD) spectroscopy to study induced secondary structure of the peptide in various solvent systems, including phospholipid vesicles and a detergent.

Abbreviations: Apo-CII, Apolipoprotein CII; CD, Circular Dichroism; DOPC, 1,2-dioleoyl-*sn*-glycero-3-phosphocholine; DOPG, 1,2-dioleoyl-*sn*-glycero-3-phosphoglycerol; HAc, Acetic Acid; HFP, 1,1,1,3,3,3-hexafluoro-2-propanol; ISPA, Isolated Spin Pair Approximation; NMR, Nuclear Magnetic Resonance; NOE, Nuclear Overhauser Enhancement; NOESY, Nuclear Overhauser Enhancement Spectroscopy; RMSD, Root Mean Square Deviation; SDS, Sodium Dodecyl Sulfate.

Correspondence to: A. Gräslund

Materials and methods

Structure calculations

The initial structures of the fragment of apo-CII were calculated based on the isolated spin pair approximation (ISPA) approach using the distance geometry program DIANA (Güntert et al. 1991), obtained from K. Wüthrich, ETH, Zürich. Generated structures were refined with the extended version of XPLOR, version 2.1 (Brünger 1990), obtained from A. Brünger, Yale University, New Haven. XPLOR enables distance-based refinement (using the ISPA) as well as relaxation matrix refinement. Processing of spectra and peak intensity determination were performed on a Sun 3/260 workstation. A Silicon Graphics 4D/25G workstation was used for the structure calculations. The graphics program HYDRA was obtained from R. Hubbard, University of York, England.

Processing of spectra

The NMR data were acquired as previously described (Lycksell et al. 1992). Processing of spectra was made with the NMR*i* software program nmr2. Prior to Fourier transformation the data in the t_1 dimension were zerofilled to 1024 points, since each of the 512 t_1 increments contained 1024 real data points. The transition to the zerofilling was smoothed with a so called roll off function. Distortions in the base plane were adjusted by a base-flattening routine.

Integration of NOESY crosspeaks was made with the surface fitting routine in the nmr2 software system. For large crosspeaks the uncertainties in the calculated intensities were rather small (5–15% – standard deviation), but were considerably larger ($\sim 25\%$) for small or overlapping peaks and also for peaks in noise ridge regions. The number of integrated peaks varied with the spectrum mixing time from 125 to 200.

Distance constraints

The NOESY crosspeak build-up rates were converted to proton-proton distances, where the distance between HA of Ser73 and HN of Val74 was used as reference. In a model α-helix this distance is 3.5 Å. Since these residues are located in the backbone of a proposed well-defined α-helical region (Lycksell et al. 1992), their crosspeak build-up rate was taken to correspond to 3.5 Å. Choosing this reference distance gave, for most residues, intra-residue HA and HN proton distances between 2.8 and 3.0 Å, as expected for α-helical and extended regions. This indicates that one of these distances could equally well have been chosen as a reference. It was not possible to use an intra-residue reference distance involving a side-chain proton since the side-chains have different mobility compared to the backbone, giving rise to unphysical distances for the backbone.

The distance constraints used were a lower limit of 2 Å and an upper limit given by the calculated distance plus a term of 0.5 Å added. The upper limits were also corrected for the use of pseudoatoms, where the corrections used were the ones suggested in (Wüthrich 1986). A total number of 244 constraints were used. Of these there were 125 inter-residue, but none between residues more than 4 residues apart.

Distance geometry

We used the program DIANA (Güntert et al. 1991) which varies the dihedral angles about rotatable bonds and minimizes a so called variable target function. Only upper and lower bounds of proton-proton distance limits were used. The minimization was performed in eleven stages. The initial stages included only local constraints. In the following stages longer interactions were gradually introduced. One hundred structures were generated from one hundred different random starting structures, where the 244 constraints applied were the ones described above.

Structure refinement

Following distance geometry calculations, energy minimization and restrained molecular dynamics were performed with the program XPLOR (Brünger 1990). The energy function used in this program is a combination of empirical and experimental information, as follows:

$$E_{\text{total}} = E_{\text{empirical}} + E_{\text{experimental}}.$$

In order to maintain ideal geometry of the molecule during the refinement, the energy function $E_{\text{empirical}}$ is calculated from the provided topology and parameter set topallhsa.pro and parallhsa.pro which have been developed especially for this purpose (Brünger 1990). This reflects the fact that the purpose is not to describe the dynamics of the protein, but to determine the structural properties.

The part of this energy function which takes the experimental data into consideration is the term $E_{\text{experimental}}$. It can be calculated according to the isolated spin pair approximation or from the NOE intensities, via the full relaxation matrix, or as a combination of both. In both cases a flat-bottomed square well potential was used to incorporate the distance constraints and the NOESY intensities, described by Nilges (Nilges et al. 1988, 1991).

The well potential function used in the refinement against NOE intensities is defined as the absolute value of the difference between the calculated and observed crosspeak intensities, where the observed crosspeaks have individual error estimates as described above. Calibration factors were recalculated every 0.5 ps during the refinement. The tolerance was set to 0.05 Å and the distance cutoff value to 4.5 Å. According to Nilges (Nilges et al. 1991) these should be appropriate values.

A way of describing the quality of a structure calculation is by using the NMR R-factor. The R-factor describes the fit between the theoretical NOE intensities, obtained by back-calculation from the calculated structure, and the experimentally observed NOE intensities. It is correlated with the energy potential via the well potential function,

which drives the change of the structure of the molecule in the molecular dynamics simulations (Nilges et al. 1991). Questions about the use of the NMR R-factor have been raised (Withka et al. 1992), but for our purpose it seems appropriate.

Methyl groups are represented by one spin and the distance to such a group is calculated using $\langle r^{-3} \rangle^{-1/3}$ averaging as suggested (Koning et al. 1990). Using empirical methods (short simulations) the energy constants for the relaxation matrix term, K_{relax}, was set to 200 kcal $\cdot$ mol$^{-1} \cdot$ Å^{-2} and the distance based term, K_{noe}, to 50 kcal $\cdot$ mol$^{-1} \cdot$ Å^{-2}. In the restrained molecular dynamics simulations, using distance constraints, a timestep of 1 fs was used. When the refinement was done with the incorporation of the relaxation matrix the timestep used was 0.5 fs. Initial velocities were chosen from a Maxwellian distribution at specified temperatures and rescaled at appropriate time intervals. The covalent bonds of hydrogen atoms were constrained with the SHAKE algorithm (Ryckaert et al. 1977) in all stages except during the final 10 ps of the molecular dynamics simulations (protocol 1, see below) and during the final minimizations (protocols 2 and 3). The default values were chosen for the nonbonded parameters.

Refinement strategy

Three different kinds of refinement strategies were used. The first protocol only used distance constraints and consisted of an initial minimization followed by a 20 ps molecular dynamics simulation where the temperature was 800 K during the first 6 ps and was then lowered to 298 K during the rest of the simulation.

The second protocol is initially similar to the first one but continues with a 5 ps molecular dynamics simulation using NOESY intensity constraints followed by a final minimization.

The third protocol is a refinement against NOESY intensities, as follows:

a) 25 steps of minimization, $K_{relax} = 40$ kcal $\cdot$ mol$^{-1} \cdot$ Å^{-2}.
b) Molecular dynamics in 0.5 ps at the temperature 298 K. K_{relax} was increased with 40 kcal $\cdot$ mol$^{-1} \cdot$ Å^{-2} every 0.125 ps to reach the final value of 200 kcal $\cdot$ mol$^{-1} \cdot$ Å^{-2}.
c) Molecular dynamics in 3 ps, $K_{relax} = 200$ kcal $\cdot$ mol$^{-1} \cdot$ Å^{-2}.
d) 100 steps of minimization on an average structure calculated from the final 0.5 ps of the molecular dynamics trajectory, $K_{relax} = 200$ kcal $\cdot$ mol$^{-1} \cdot$ Å^{-2}.

In refinement protocol 1, ten distance geometry structures with the lowest target functions were used as starting structures. Refinements using protocols 2 and 3 were performed with only 3 starting structures, owing to the CPU time consumption.

Circular dichroism spectroscopy

Apo-CII fragment solutions with a concentration of approximately 30 μM were titrated with HFP and sodium dodecyl sulfate (SDS) as well as vesicle solutions prepared from 1,2-dioleoyl-*sn*-glycero-3-phosphocholine (DOPC) and 1,2-dioleoyl-*sn*-glycero-3-phosphoglycerol (DOPG). The induced conformational change was monitored by CD-spectroscopy. In the titration with SDS a 10 mM HAc solution was used, in all other cases water was used.

SDS was purchased from BDH Limited Poole, England, and HFP from SIGMA. DOPC and DOPG were purchased from Avanti Polar Lipids (U.S.A.). Stock solutions of 5.0 mg/ml of DOPC and DOPG unilamellar lipid vesicles were produced by sonication as previously described (Kalman et al. 1989 and references cited therein). The sonicator used was a Soniprep 150 (MSE, Scientific Instruments, England) supplemented with an exponential microtip.

CD-spectra were recorded using a Jasco-720 spectropolarimeter, 2 mm Hellma quartz cuvettes, at a temperature of 25 °C. Spectra were corrected with respect to baseline and for dilution.

Results

Structures generated by distance geometry

Distance geometry calculations were used to generate one hundred different structures of the 50–79 fragment of apo-CII. Among the ten structures with the lowest target functions the number of violated constraints was very low (from 3 to 11 of a total of 244) and with a maximum violation of 1 Å or less. The R-factors for these structures assumed values around 1.

It is clear that the region between residues 67 and 74 forms a well defined helix structure. This is illustrated in Fig. 1 where the ten structures are shown with residues 67 to 74 matched for best fit. The ends and a region around Gly 65 seem not to adopt a specific conformation, probably due to lack of distance constraints in these regions. For the regions spanned by residues 56 to 59 and 74 to 77 slightly more well defined conformations are seen.

Refinement of distance geometry structures

The distance geometry structures with the lowest target function were chosen as starting structure for the refinement calculations. The refinement was made with the program XPLOR and included energy minimization as well as molecular dynamics in accordance with the protocols discussed above. An important parameter in the molecular dynamics refinement, using NOE intensities as constraints, is the rotation correlation time. It can be estimated for a globular molecule with isotropic motion in water solution (Cantor and Schimmel 1980) to be about 1.4 ns for a molecular weight of 3.3 kDa. The initial distance geometry structure of the apo-CII fragment has an elongated form, which means that this system is anisotropic, and better represented with at least two rotational correlation times. This would mean a more complicated computational task which requires a large amount of NOE data of high accuracy. However, the amount of data

Fig. 1. 10 superimposed backbone structures of the apo-CII fragment, calculated by the distance geometry program DIANA, using distance constraints from proton NMR (NOESY) data. The structures were fitted to minimize the RMSD for the backbone atoms of residues 67 to 74

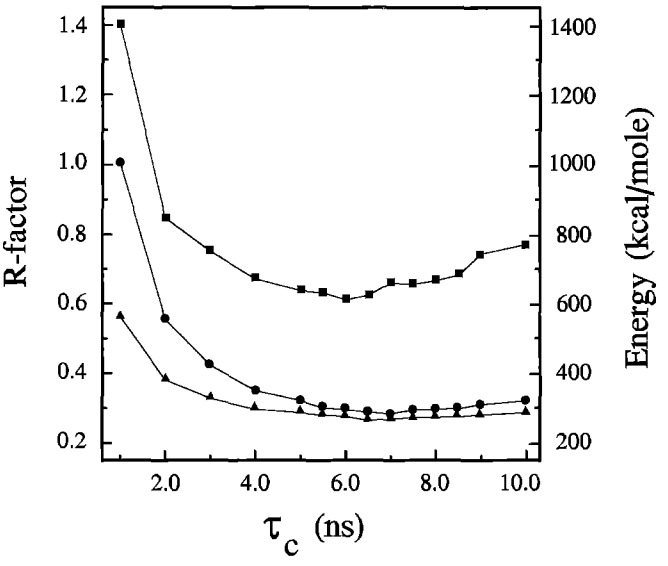

Fig. 2. The dependence of the rotational correlation time for the total energy (*squares*) and the NOE-energy (*triangles*) of the system as well as the R-factor (*circles*). These results are based on short molecular dynamics simulations (25 fs) at different rotational correlation times using intensity constraint from the NOESY spectrum at a mixing time of 135 ms

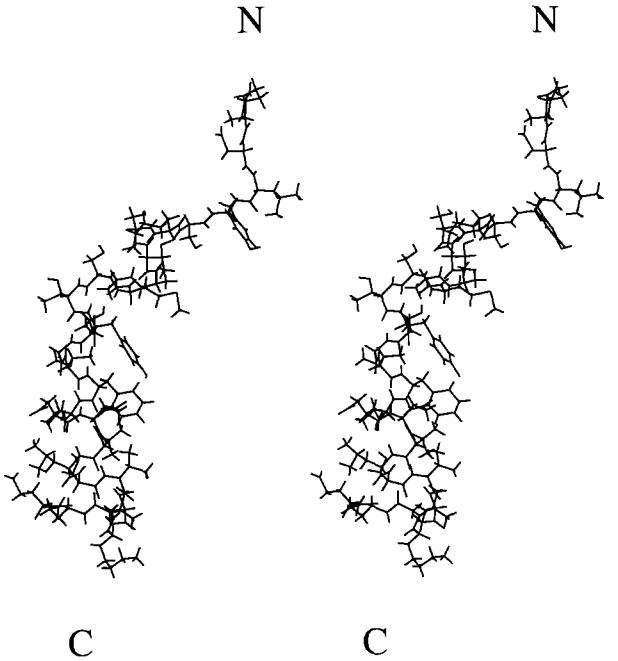

Fig. 3. A stereo view of the refined apo-CII fragment structure, including all atoms

in this work makes it reasonable to use only a single rotational correlation time, which presumably is longer than for a globular protein of the same size. Results from viscosity measurements, using a capillary viscosimeter (data not shown), shows that the rotational correlation time for the fragment in this solvent should be around 3–4 ns. Several short molecular dynamics simulations (25 fs) with intensity constraints from the NOESY spectrum at a mixing time of 135 ms were performed using varying rotational correlation times. A plot of the energy of the molecule as well as the R-factor versus the rotational correlation time is shown in Fig. 2 and suggests a "best fitting" rotational correlation time of at least 4 ns. Based on these considerations and results the rotational correlation time in a 35%/65% mixture of HFP and water of the apo-CII fragment was chosen as 4 ns for the structural refinement calculations.

The R-factors as well as RMSD-values after the structure refinement calculations with the protocols described above are presented in Tables 1 and 2. A more detailed analysis was made on the structure generated with protocol 3. During the simulation the R-factor reached an equilibrium value after about 1 ps. No obvious effects were seen of the R-factor calibration, which took place every 0.5 ps.

A stereo view, including all atoms of the structure after the relaxation matrix refinement is shown in Fig. 3. The C-terminal helix can be distinguished quite easily and also a number of hydrophobic residues gathered on one side of the helix, indicating an amphiphatic character of the helix. A view along the helix, showing the backbone atoms, can be seen in Fig. 4. Another turn of helix is also seen in the N-terminal part.

A Ramachandran plot for this structure, which shows the dihedral angles along the polypeptide chain, was calculated and is shown in Fig. 5. The solid contour lines indicate areas sterically allowed for an alanyl polypeptide chain (Ramachandran et al. 1963).

Effects of solvents on secondary structure

CD spectroscopy was used to probe the influence of various solvent conditions on the secondary structure of the peptide fragment. Fig. 6 shows CD spectra obtained in the presence of DOPC and DOPG vesicles, 10 mM SDS/10 mM HAc and 35% HFP. A close coincidence is observed between the spectra obtained in SDS and 35% HFP, with a considerable negative amplitude at 222 nm, indicative of the presence of α-helix. The neutral (DOPC) or negatively charged (DOPG) phospholipid vesicles only marginally affect the random-like structure that is also apparent in aqueous solution (Lycksell et al. 1992).

In titrations with HFP we found that addition of HFP leads to an approximately proportional increase of the negative 222 nm amplitude up to 85% HFP. There was no absolute isobestic point in the titration. This indicates that more than two conformational states are present. At 85% HFP concentration the specific ellipticity at 222 nm corresponds to almost 66% α-helix. In the 35% HFP aqueous solvent, the α-helical content is estimated as 36%. This corresponds reasonably well with the determined NMR structure, which has about 40% α-helical structure. In the titration with SDS, addition of 5 mM SDS, corresponding to a peptide:SDS ratio of 1:170, led to an immediate change of the CD spectrum, which then remained unchanged after addition of more SDS (data not shown).

Table 1. R-factors for different regions of the structures of the 50–79 fragment of apolipoprotein CII, generated by different methods. As starting structure the distance geometry structure with the lowest target function was used. A few abbreviations have been used: DG – distance geometry, DG → MD-distance geometry followed by restrained molecular dynamics, DG → MD → REL-distance geometry followed by restrained molecular dynamics and refinement with the full relaxation matrix, DG → REL-distance geometry followed by refinement with the full relaxation matrix

Method of calculation	R-factor			
	Region			
	50–79	56–59	67–74	74–77
DG	0.93	0.48	0.57	0.48
DG → MD	0.84	0.50	0.55	0.44
DG → MD → REL	0.35	0.24	0.25	0.30
DG → REL	0.34	0.21	0.23	0.32

Discussion

To describe the quality of a well-ordered solution structure determined by NMR, RMSD values between pairs of structures in an ensemble, and R-factors, describing the fit between calculated and experimental NOE intensities, are commonly used (Nikonowicz et al. 1990, Edmonson et al. 1991, Thomas et al. 1991, Nilges et al. 1991). While

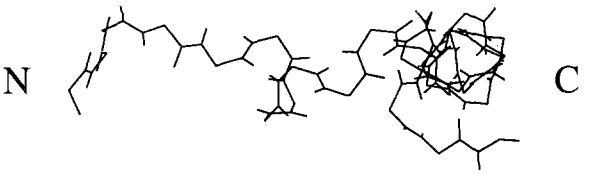

Fig. 4. A view through the α-helix of the refined apo-CII fragment structure, showing only backbone atoms

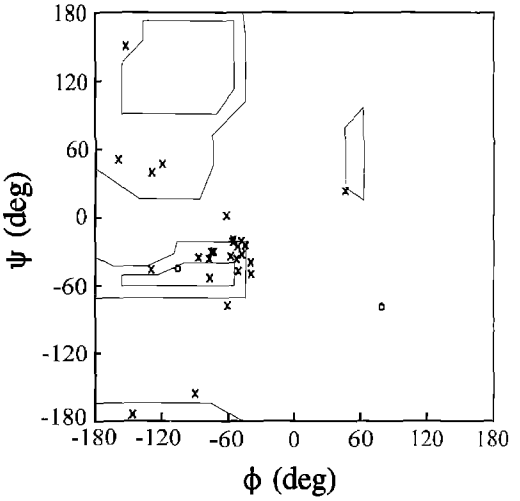

Fig. 5. A Ramachandran plot of the peptide bond dihedral angles ϕ and ψ in the refined structure of the apo-CII fragment. The two glycines are indicated by rings (o) and all other residues by crosses (×). The solid contour lines indicate areas sterically allowed for an alanyl polypeptide

Table 2. Energy characteristics and RMSD-values for structures of the 50–79 fragment of apolipoprotein CII, generated by different methods. As starting structure the distance geometry structure with the lowest target function was used. The RMSD-values were calculated for different parts of the fragment and involved backbone atoms. A few abbreviations have been used: DG → MD-distance geometry followed by restrained molecular dynamics, DG → MD → REL-distance geometry followed by restrained molecular dynamics and refinement with the full relaxation matrix, DG → REL-distance geometry followed by refinement with the full relaxation matrix

Method of calculation	RMSD (Å)				Energy		
	Region				(kcal/mol)		
	50–79	56–59	67–74	74–77	Total	Electrostatic	Relaxation matrix
DG → MD	9.13	0.77	0.63	0.35	7 084	−612	6 972
DG → MD → REL	9.13	1.00	0.98	0.60	274	−597	408
DG → REL	1.63	0.82	0.42	0.37	556	−350	418

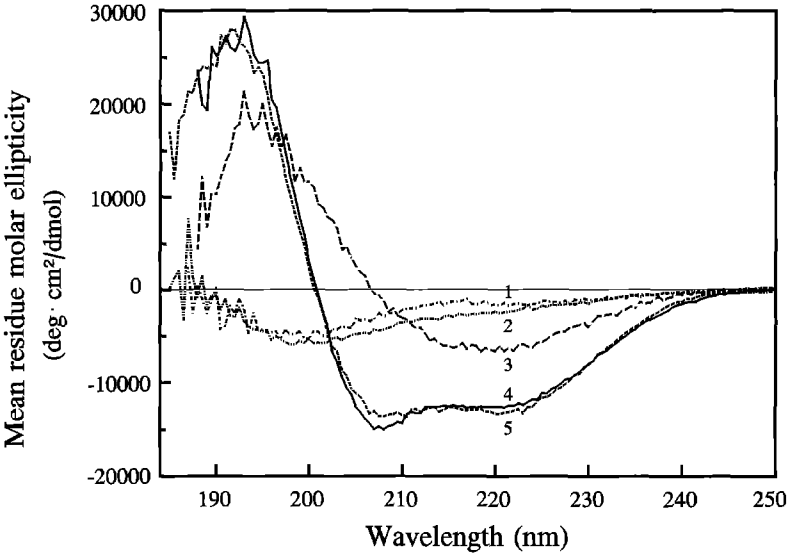

Fig. 6. Circular dichroism spectra at 25°C of the apo-CII fragment at equal concentration (30 μM) in different solvents. 1. 0.2 mg/ml DOPC; 2. water; 3. 0.2 mg/ml DOPG; 4. 10 mM SDS/10 mM HAc; 5. 35% HFP

RMSD values should measure the precision of a structure determination, the R-factor should be one way to estimate the accuracy, under conditions where there are enough experimental constraints available.

In aqueous solution, small peptides would be expected to have several conformers. For the NMR study of the apo-CII fragment we had the strategy to use solvent conditions that would mimic an amphiphilic environment and stabilize the peptide structure. The stability of the structure of certain regions of the apo-CII fragment was well documented from exchange studies of the amide protons, which exchanged on the timescale of days (Lycksell et al. 1992). The inter-residue resonances, which are important for generating a three-dimensional structure, were mainly found in these regions. Based on these experimental conditions it should be reasonable to use an R-factor to optimize the quality of the determined structure. The present results show that the structure of the stable parts of the fragment can be well determined by refinement calculations.

It was clear that the distance constraints were easily fulfilled with the distance geometry calculations, with almost no large violations. The R-factors were however large, i.e. the agreement between calculated and observed NOESY crosspeak intensities was rather poor.

When molecular dynamics with distance constraints was performed, a large improvement of the energy of the system was seen as well as an ability to change the structure considerably (Table 2). However, only a slight improvement of the R-factors was seen (Table 1), probably due to the fact that the rather liberal distance constraints are already fulfilled by the distance geometry calculations.

The largest improvement of the R-factors was seen when relaxation matrix refinement was introduced. Almost half of the improvement can be attributed to energy minimization. This refinement was done using starting structures both directly from a distance geometry structure as well as from a structure generated with molecular dynamics using distance constraints. Differences in the conformation between these cases were seen in particular around residue Gly-65, which is not well-defined by NOE constraints. These different approaches help us to identify the three different parts of the apo-CII protein fragment which remain almost unchanged and thus have a well-defined structure (Table 2).

The present structure (Figs. 3 and 4) is the best distance geometry structure refined using the full relaxation matrix, protocol 3. The Ramachandran plot showed that protocol 3 made the dihedral angles adopt values which were in the allowed regions.

In the presented structure a well defined helix between residues 67 and 74 is obvious and was seen already after the distance geometry calculations, see Fig. 1. A detailed analysis of the structural parameters after the simulation shows that the distances and the dihedral angles have values which correspond closely to those of an α-helix. In the Ramachandran plot (Fig. 5) it is shown that most of the backbone dihedral angles, except for those at the ends of the molecule and those around residue 65, are located in the region typical for an α-helix. It is also clear that the α-helix has a slightly amphipathic character, since the hydrophobic residues 67, 71, 74 and 75 are positioned on what turns out to be the same side of the helix.

The second part of the protein which adopts a reasonably well-defined conformation, comprises residues 56 to 59. The analysis makes it clear that it is one turn of an α-helix. A third rather well-defined structured region appears on the C-terminal side of the α-helix between residues 74 and 77. This is a β-turn-like structure.

The overall model of the molecule is that of a rather extended and flexible chain with well structured parts, separated by a disordered region around Gly 65. This aspect of the structure appears best in the superposition of distance geometry structure (Fig. 1). On the other hand the regularities in the well ordered parts appear more clearly in the relaxation matrix refined structure (Figs. 3 and 4). The flexibility of the molecule inevitably limits the amount of three-dimensional structure that can be determined in solution.

The CD results, in 35% HFP, show 35% α-helical character of the secondary structure. The NMR data

shows that about 12 out of 30 residues (i.e. 40%) appear in α-helical conformation. This fact supports a high degree of population of the calculated structures.

From the literature (Wang 1991 and references cited therein) it is known that residues 56 to 79 are important for the activation of lipoprotein lipase. According to a Chou-Fasman prediction (Mantulin et al. 1980) this part should adopt a β-sheet structure, which is in sharp contrast to the results presented here. In our results the predominant secondary structure is a remarkably stable α-helix with an amphipathic character spanning approximately residues 67 to 74, which could be of importance for the interaction of apo-CII with lipoprotein lipase.

The results of the CD studies (Fig. 6) show that 35% HFP in aqueous solution induces an average secondary structure very similar to the one induced by SDS. Phospholipid vesicles, whether neutral or negatively charged, have on the other hand, a very small effect on the CD results. These observations agree with previous studies showing that residues 50 to 79 of apo-CII are not directly involved in binding to the lipoprotein particles or phospholipid membranes (Sparrow and Gotto 1980). This function has rather been suggested to be found in the N-terminal part (1–49) of intact apo-CII.

The 50–79 fragment should provide the site for interaction with lipoprotein lipase in an environment of unknown degree of hydrophobicity. Our results shows that interactions with more hydrophobic molecules such as HFP or SDS induce a rather well ordered structure which might be the one recognized by the lipase.

Acknowledgements. We thank L. B.-Å. Johansson for his useful suggestions and E. Vikström for preparing the lipid vesicle solutions. We are also grateful to J. Zdunek for letting us use his graphical program PROGRAPH. This study was supported by the Swedish Natural Science Research Council and the Magn. Bergvall Foundation.

References

Brünger AT (1990) XPLOR manual (Version 2.1). Yale University, New Haven

Cantor CR, Schimmel PR (1980) Biophysical chemistry, part II. Freeman, New York

Edmonson S, Khan N, Shriver J, Zdunek J, Gräslund A (1991) The solution structure of motilin from NMR distance constraints, distance geometry, molecular dynamics, and an iterative full relaxation matrix refinement. Biochemistry 30:11271–11279

Güntert P, Braun W, Wüthrich K (1991) Efficient computation of three-dimensional protein structures in solution from nuclear magnetic resonance data using the program DIANA and the supporting programs CALIBA, HABAS and GLOMSA. J Mol Biol 217:517–530

Kalman B, Johansson LBÅ, Lindberg M, Engström S (1989) Electronic energy transfer in anisotropic systems. 2. 2,5,8,11-tetra-*tert*- butylperylene in vesicles. J Phys Chem 93:8371–8376

Koning TMG, Boelens R, Kaptein R (1990) Calculation of the nuclear overhauser effect and the determination of proton-proton distances in the presence of internal motions. J Magn Reson 90:111–123

Lycksell P-O, Öhman A, Bengtsson-Olivecrona G, Johansson LBÅ, Wijmenga SS, Wernic D, Gräslund A (1992) Sequence specific ^{1}H-NMR assignments and secondary structure of a carboxy-terminal functional fragment of apolipoprotein CII. Eur J Biochem 205:223–231

Mantulin WW, Rohde MF, Gotto Jr AM, Pownall HJ (1980), The conformational properties of human plasma apolipoprotein C-II. J Biol Chem 255:8185–8191

Nikonowicz EP, Meadows RP, Gorenstein DG (1990) NMR structural refinement of an extrahelical adenosine tridecamer d(CGCAGAATTCGCG)$_2$ via a hybrid relaxation matrix procedure. Biochemistry 29:4193–4204

Nilges M, Clore GM, Gronenborn AM (1988) Determination of three-dimensional structures of proteins from interproton distance data by hybrid distance geometry-dynamical simulated annealing calculations. FEBS Lett 229:317–324

Nilges M, Habazettl J, Brünger AT, Holak TA (1991) Relaxation matrix refinement of the solution structure of squash trypsin inhibitor. J Mol Biol 219:499–510

Ramachandran GN, Ramakrishnan C, Sasisekharan V (1963) Stereochemistry of polypeptide chain configurations. J Mol Biol 7:95

Ryckaert J-P, Ciccotti G, Berendsen HJC (1977) Numerical integration of the carteesian equations of motion of a system with constraints: molecular dynamics of n-alkenes. J Comput Phys 23:327–341

Sparrow JT, Gotto AM Jr (1980) Phospholipid binding studies with synthetic apolipoprotein fragments. Ann NY Acad Sci 348:187–211

Thomas PD, Basus VJ, James LJ (1991) Protein solution structure determination using distances from two-dimensional nuclear overhauser effect experiments: Effect of approximations on the accuracy of derived structures. Proc Nat Acad Sci, USA 88:1237–1241

Wang Chi-Sun (1991) Structure and functional properties of apolipoprotein CII. Prog Lipid Res 30:253–258

Withka JM, Srinivasan J, Bolton PH (1992) Problems with, and alternatives to, the NMR R-factor. J Magn Reson 98:611–617

Wüthrich K (1986) NMR of proteins and nucleic acids. Wiley, New York